THE JOURNAL OF PHYSICAL CHEMISTRY C

Article

Cite This: J. Phys. Chem. C 2018, 122, 25829−25836

pubs.acs.org/JPCC

Computational Study of $NaVOPO_4$ Polymorphs as Cathode Materials for Na-Ion Batteries: Diffusion, Electronic Properties, and Cation-Doping Behavior

Pablo A. Aparicio,*[,†] James A. Dawson,[‡] M. Saiful Islam,*[,‡] and Nora H. de Leeuw*[,†]

[†]School of Chemistry, Cardiff University, Main Building, Park Place, Cardiff CF10 3AT, United Kingdom

[‡]Department of Chemistry, University of Bath, Bath BA2 7AY, United Kingdom

Supporting Information

ABSTRACT: Rechargeable sodium-ion batteries have gained considerable interest as potential alternatives to lithium-ion batteries, owing to their low cost and the wide abundance of sodium. Phosphate compounds are promising materials for sodium-ion batteries because of their high structural stability. Vanadium phosphates have shown high energy densities as cathode materials, but their Na-ion transport and cation-doping properties are not as yet fully understood. Here, we have combined density functional theory calculations and molecular dynamics techniques to study the diffusion, electronic properties, and cation doping of the α-, β-, and α_I-$NaVOPO_4$ polymorphs. The calculated Na-ion activation energies of these compounds (0.3−0.5 eV) are typical for Na-based cathode materials and the simulations predict Na-ion diffusion coefficients of 10^{-11}−10^{-12} cm^2 s^{-1}. The cell voltage trends show an operating range of 3.1−3.3 V vs Na/Na^+, with the partial substitution of vanadium by other metals (Al^{3+}, Co^{2+}, Fe^{3+}, Mn^{4+}, Ni^{2+}, or Ti^{4+}) increasing the cell voltage by up to 0.2−1.0 V vs Na/Na^+. Our study provides new quantitative insights into the electrochemical behavior of a potentially important class of phosphate cathode materials for sodium-ion batteries.

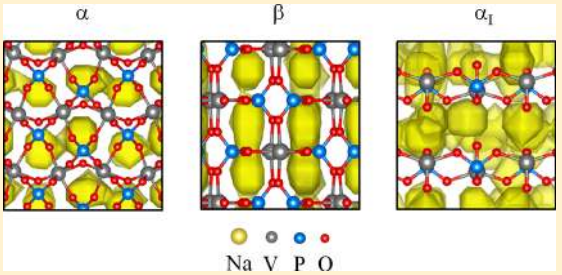

1. INTRODUCTION

The development of lithium-ion batteries has enabled a host of new technologies, particularly portable electronic devices. In recent years, sodium-ion batteries have begun to receive interest with the aim of developing low-cost and sustainable batteries based on the high abundance and easy accessibility of sodium, especially for grid-scale storage systems for intermittent renewable energy.[1−5]

Considerable effort has been expended on the exploration of new cathode materials with high reversible capacity, rapid Na insertion/extraction, and cycling durability.[3,6−8] A large variety of materials, including layered metal oxides, polyanionic compounds, and Prussian blue analogs, have been studied as cathodes for Na-ion batteries.[3,9] In particular, vanadium phosphate materials, such as $Na_3V_2(PO_4)_3$, $Na_3V_2(PO_4)_2F_3$, and $NaVPO_4F$, show good electrochemical performance and they possess a versatile structure.[10−12] They are considered promising cathode compounds owing to their high structural stability, long-term cycling, and low volumetric expansion during Na^+ insertion/extraction.[13]

Song et al. explored monoclinic α-$NaVOPO_4$ as a cathode for Na-ion batteries.[14] More recently, Manthiram and coworkers synthesized and tested two new $NaVOPO_4$ polymorphs, i.e., the β and α_I phases, both of which exhibited a higher potential and reversible capacity than the α phase.[15,16] The new β and α_I polymorphs have both been synthesized from the lithium counterparts, via delithiation and sodiation chemical processes, but it was found that the new phases are thermodynamically less stable than the α phase.

The α_I phase has the highest ionic conductivity among the three polymorphs, making it a promising cathode for Na-ion batteries, although the Na-ion transport mechanisms and electronic properties of the $NaVOPO_4$ polymorphs are not yet fully characterized. Li et al. designed a high-energy Na-ion battery based on structured $Na_2Ti_3O_7$ and layered α_I-$NaVOPO_4$ compounds as the anode and cathode materials, respectively.[17] This cell battery showed excellent reversible capacity, rate capability, and cycling stability. Lin et al.[18] published a comparison of $VOPO_4$ polymorphs investigating their stability and electrochemistry of Li and Na intercalation.

Here, we report the diffusion, electronic properties, and cation doping of the α-, β-, and α_I-$NaVOPO_4$ polymorphs studied by an effective combination of ab initio calculations and classical molecular dynamics (MD) simulation techniques. We were able to reproduce the experimental structural parameters of the three polymorphs. The Na-ion transport mechanisms and voltage trends from metal doping were also investigated and the doped structures show an increase in the cell voltage of up to 0.2−1.0 V vs Na/Na^+. We found that the α_I phase has the highest Na-ion diffusion coefficient and the

Received: August 10, 2018
Revised: September 28, 2018
Published: October 2, 2018

DOI: 10.1021/acs.jpcc.8b07797
J. Phys. Chem. C 2018, 122, 25829−25836

lowest activation energy for Na-ion migration among the three polymorphs.

2. METHODS

We have employed a combination of ab initio techniques based on density functional theory (DFT) and interatomic potential-based molecular dynamics (MD) simulations, extending our successful work on related battery materials.[19−25] All DFT calculations were performed using the Vienna ab initio simulation package (VASP).[26−29] We have used projector-augmented wave pseudopotentials[30,31] and the Perdew−Burke−Ernzerhof exchange correlation functional revised for solids (PBEsol),[32] setting the kinetic energy cut-off at 520 eV. A k-point grid of 7 × 7 × 7 was used to converge the forces and energies of the bulk material. The DFT+U methodology was applied to account for the d orbitals of the metal atoms, with effective Hubbard values of $U_{eff} = U - J$ = 4.0, 3.3, 4.3, 3.9, 6.0, and 4.2 eV (J = 1 eV) for V, Co, Fe, Mn, Ni, and Ti, respectively.[11,33,34] In addition, van der Waals corrections were included, using the DFT-D3 method of Grimme,[35] as these have been shown to influence cell voltage calculations in some polyanionic systems.[19]

Previous computational studies have shown that such methods are suitable to compute accurate cell voltage trends[20] as well as to determine transport and defect properties in Li- and Na-ion batteries.[36−38] For all compounds, the cell voltage vs Na/Na^+ of the V^{4+}/V^{5+} redox couple was calculated using the following equation

$$V = E[NaVOPO_4] - E[VOPO_4] - \mu[Na] \quad (1)$$

where $E[NaVOPO_4]$ and $E[VOPO_4]$ are the total energies of the $NaVOPO_4$ and $VOPO_4$ structures, respectively. The chemical potential of sodium, μ[Na], was calculated using metallic sodium, which is the standard practice for cell voltage calculations. We also used eq 1 to compute the cell voltage vs Na/Na^+ of the $NaV_{1-x}M_xOPO_4$ doped compounds, where we assumed that the fully desodiated structures ($V_{1-x}M_xOPO_4$) can be formed.

The MD simulations were performed with the LAMMPS code[39] and the calculations were carried out on a large supercell made up of 7 × 7 × 7 unit cells, consisting of 10 976 atoms. The initial configuration of the supercell contained 10% Na vacancies plus corresponding V^{5+} species, which were randomly distributed. Pre-equilibrium runs of 4 ps using a time step of 2 fs with the NPT ensemble (constant number of particles, constant pressure, and constant temperature) were first used to obtain stable configurations. Data collection runs were then carried out using the NVT ensemble (constant number of particles, constant volume, and constant temperature) and a time step of 1 fs for long runs of 10 ns, at temperatures in the range of 300−1400 K. The interatomic potentials used in the MD calculations are listed in Table S1. The mean squared displacement (MSD) of the Na ions was computed first to derive the diffusion coefficients (D_{Na}) according to

$$D_{Na} = \left(\frac{1}{6t}\right)\langle [r(t)]^2 \rangle \quad (2)$$

where t is time and $\langle [r(t)]^2 \rangle$ is the MSD.

3. RESULTS AND DISCUSSION

3.1. Structural and Electronic Analysis. Lii et al. first reported the synthesis and structural characterization of $NaVOPO_4$.[40] The magnetic behavior of this compound was described by O'Connor et al. as anti-ferromagnetically coupled S = 1/2 one-dimensional (1D) chains[41] with the structure of the α-$VOPO_4$ polymorph. Vanadyl phosphate ($VOPO_4$) crystallizes in several different structures, namely as $\alpha/\alpha_I/\alpha_{II}$, β, γ, δ, ε, and ω-$VOPO_4$.[42−48] So far, only three sodium-containing products have been synthesized: α (monoclinic),[40] β (orthorhombic),[15] and α_I (tetragonal)[16] $NaVOPO_4$.

The α structure of $NaVOPO_4$ consists of VO_6 octahedral chains running along the c axis, linked with PO_4 tetrahedra (Figure 1). The VO_6 octahedra show four almost equal V−O bond distances in the equatorial plane (1.97−2.01 Å), and one short and one long apical V−O distances (1.68 and 2.09 Å, respectively). Three of the four P−O bond distances in the PO_4 tetrahedra are similar (1.56−1.58 Å), whereas the other distance is slightly shorter (1.52 Å). The Na^+ cations are in the intersections of the VO chains, surrounded by seven O atoms with Na−O distances ranging from 2.25 to 2.92 Å.

In the β phase, distorted VO_6 octahedra form infinite chains along the a axis, while the V−O bonds in the bc planes are connected via shared corners with four PO_4 tetrahedra (Figure 1). Short (1.64 Å) and long (2.37 Å) V−O distances alternate along the a axis to form the vanadyl-type symmetry. The V−O bonds in the equatorial plane are in the range of 1.93−2.06 Å. As in the α phase, three of the P−O bonds in the PO_4 tetrahedra have similar bond lengths (1.55−1.56 Å), with the other one being slightly shorter (1.53 Å). The Na^+ cations are surrounded by six O atoms with Na−O distances ranging from 2.23 to 2.36 Å.

Finally, the α_I-$NaVOPO_4$ structure consists of $VOPO_4$ sheets stacked along the c direction. In the $VOPO_4$ planes, PO_4 groups and distorted VO_5 polyhedra are alternatively arranged by a corner-sharing oxygen to form $[VOPO_4]_\infty$ chains in the ab plane (Figure 1). The VO_5 square-pyramidal groups show four equal V−O distances (1.99 Å) and a short apical vanadyl distance (1.63 Å). They also show a very long sixth V−O distance (3.48 Å). In the case of the PO_4 groups, all of the P−O distances are equal (1.55 Å). The Na cations are located between the $VOPO_4$ sheets and surrounded by six O atoms with Na−O distances ranging from 2.30 to 2.55 Å.

A comparison between the experimental and computed cell parameters and bond lengths can be found in Table 1 (all bond lengths are given in Table S2). The computed values are within 1% of the experimental values, except in the case of the α_I phase. In this case, the experimental values are not available for the $NaVOPO_4$ stoichiometry and are referred to as the α_I-$Na_{0.8}VOPO_4$ compound; hence, the computed cell parameters and bond lengths are slightly different from the experimental data. The interlayer distance between the $VOPO_4$ sheets in the α_I phase can vary up to 0.6 Å depending on the Na loading.

Turning to the electronic structure, the density of states (DOS) of the α phase is shown in Figure 2. The DOS of the β and α_I phases, which are similar to the DOS of the α phase, can be found in Figure S1. As the $NaVOPO_4$ compounds are described as anti-ferromagnetically coupled chains,[40,41] the compounds have a zero total spin and the DOS are symmetric. The electronic structure corresponds to one unpaired electron per V═O formula unit and the vanadyl chains show short-range anti-ferromagnetic exchange in the crystal lattice.

DOI: 10.1021/acs.jpcc.8b07797
J. Phys. Chem. C 2018, 122, 25829−25836

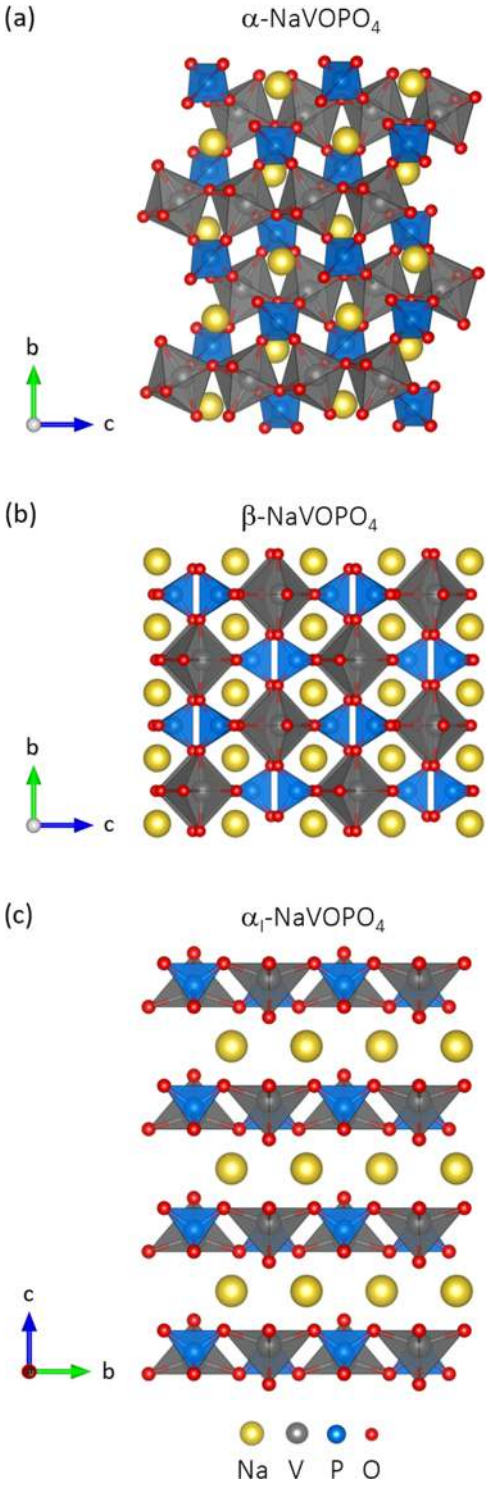

Figure 1. Polyhedral representations of the (a) α-, (b) β-, and (c) α_I-$NaVOPO_4$ polymorphs showing VO_6 octahedra (in α and β phases), VO_5 units (in α_I phase), and PO_4 tetrahedra in all phases.

Although we model the magnetic state as determined experimentally, a detailed analysis of the magnetic properties is not the focus of this study.

The valence band is described mainly by V 3d and O 2p states, whereas the conduction band is mainly made up of V 3d states. The P atoms have a relatively small contribution to both valence and conduction bands. Below the Fermi level, from −0.5 to 0.0 eV, the total DOS shows a similar contribution from the V 3d and the O 2p states, which correspond to the short V═O bonds. The band gaps of the sodiated compounds are in the range of 1.5−2.5 eV, whereas the values of the desodiated compounds are all similar (∼2 eV). These values are in good agreement with previous DFT+U results of different $VOPO_4$ polymorphs (1.3−2.2 eV).[49]

3.2. Na-Ion Diffusion Rates and Pathways. MD simulations were performed over long time scales to examine long-range Na-ion transport properties. Lin et al. computed the migration barriers of Na and Li ions in $VOPO_4$ polymorphs using the climbing image nudged elastic band method.[18] This practice is well established in the literature,[50,51] but it fails to capture the long-range dynamics of alkali-ion transport through the structure, which we have sought to elucidate here. From the MSD analysis, we observe that in the α phase, Na-ion diffusion takes place preferably in the a and c directions. In the case of the β phase, the b direction is preferred, in accord with experimental suggestions.[15] Finally, Na-ion diffusion in the α_I phase does not show any preferred direction, with the three directions being equally probable.

The MD simulations were performed over a range of temperatures (300−1400 K), covering a wider range than the operating temperatures of a typical battery and much wider than current experiments. At 300 K, the diffusion coefficients of the α-, β-, and α_I-$NaVOPO_4$ polymorphs were calculated as 1.3×10^{-11}, 6.7×10^{-12}, and 5.7×10^{-11} $cm^2\ s^{-1}$, respectively. To the best of our knowledge, there are no experimental diffusion coefficients of the $NaVOPO_4$ compounds for direct comparison. Nevertheless, the computed diffusion coefficients are similar to those found in other Na-ion cathode materials, such as Na_xCoO_2 (10^{-11} $cm^2\ s^{-1}$),[52] Na_xMnO_2 (10^{-11} $cm^2\ s^{-1}$),[53] and Na_2CoSiO_4 (10^{-12} $cm^2\ s^{-1}$).[54] The computed diffusion coefficients as a function of temperature can be used to derive migration activation energies (E_a) from an Arrhenius plot, as shown in Figure 3.

Ion migration activation energies of 0.35, 0.51, and 0.32 eV were derived for the α-, β-, and α_I-$NaVOPO_4$ polymorphs, respectively. These values indicate favorable Na-ion migration, especially in the α_I phase. Our findings cannot be compared with the literature as neither experimental activation energies nor conductivity studies of these compounds are available. However, these values are smaller than the activation energy in the related $NaTiOPO_4$ compound, which is 1.1 ± 0.1 eV in the temperature range of 480−800 K.[55]

Lin et al.[18] computed the migration barrier of β-$NaVOPO_4$ as 0.54 eV, which is in good agreement with our computed value of 0.51 eV. However, direct comparison is not appropriate for the α_I-$NaVOPO_4$ compound, since Lin et al. computed the migration barriers of three different 1D diffusion pathways, whereas our calculated value is for a three-dimensional (3D) diffusion pathway.

The diffusion trajectories are visualized in Figure 4 by plotting accumulated Na-ion densities, indicating the lattice sites most frequently crossed by Na ions during the MD simulations. These results confirm that Na ions are highly mobile, with all of the Na sites involved in bulk diffusion. In the case of the α phase, the Na diffusion takes place in two-dimensional (2D) channels, mainly in the b and c directions. In the β phase, the Na ions move in the 1D channels along the b axis. Finally, the α_I phase shows the highest Na mobility, taking place in the 3D channels. Our overall results showing high diffusion rates, low migration energies, and favorable 3D diffusion pathways for α_I-$NaVOPO_4$ makes this phase a

DOI: 10.1021/acs.jpcc.8b07797
J. Phys. Chem. C 2018, 122, 25829−25836

Table 1. Comparison of Computed and Experimental Cell Parameters and Bond Lengths in Å of α-, β-, and α_I-$NaVOPO_4$ Polymorphs

	α-$NaVOPO_4$		β-$NaVOPO_4$		α_I-$NaVOPO_4$	
	comp.	exp.[14]	comp.	exp.[15]	comp.	exp.[16] [a]
a	6.509	6.518	7.587	7.539	6.432	6.298
b	8.434	8.446	6.415	6.374	6.432	6.298
c	7.105	7.115	7.670	7.621	5.048	5.119
V−O	1.678	1.681	1.641	1.630	1.638	1.739
	2.000[b]	2.003[b]	1.994[b]	1.981[b]	1.992[b]	2.108[b]
	2.088	2.091	2.370	2.355	3.481	2.936
P−O	1.512	1.514	1.532	1.522	1.545[b]	
	1.568[b]	1.570[b]	1.555[b]	1.545[b]		
Na−O	2.446[b]	2.450[b]	2.229[b]	2.284[b]	2.382[b]	
symmetry	monoclinic		orthorhombic		tetragonal	
space group	$P2_1/C$		*Pnma*		*P4/nmm*	

[a]Cell parameters and bond lengths of α_I-$Na_{0.8}VOPO_4$ polymorph. The P−O and Na−O distances have not been reported. [b]Mean values.

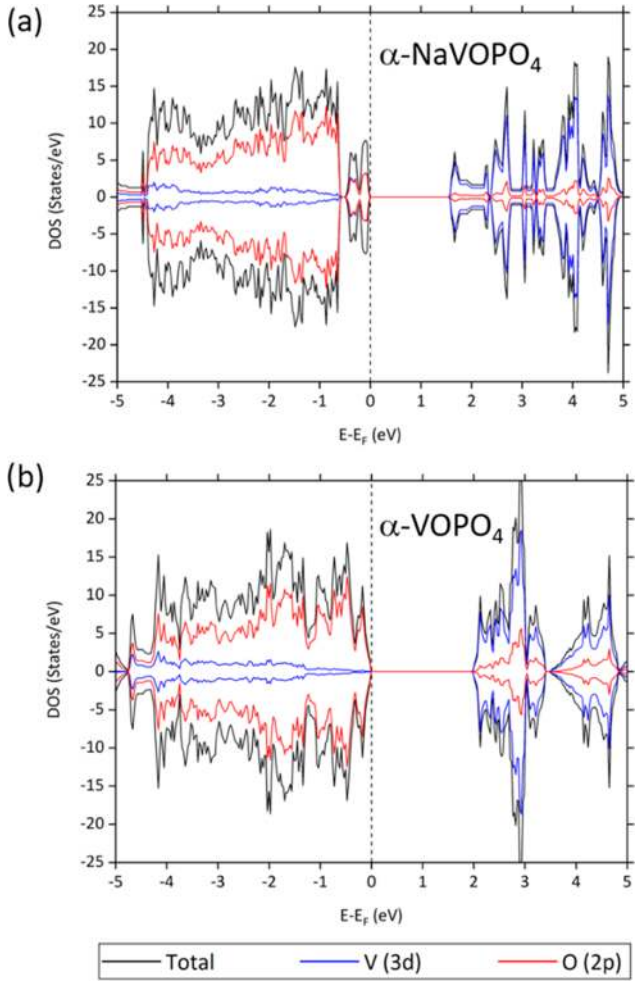

Figure 2. Density of states (DOS) of (a) sodiated α-$NaVOPO_4$ and (b) desodiated α-$VOPO_4$.

promising Na-ion cathode material. We recognize the stability issues with the α_I phase, but we consider that our predictions certainly warrant further electrochemical investigation of this promising material.

3.3. Cell Voltage Trends on Cation Doping. DFT+U was used to compute the cell voltage of the α-, β-, and α_I-$NaVOPO_4$ polymorphs as well as the doped materials. To carry out the calculations, Na ions were removed from the

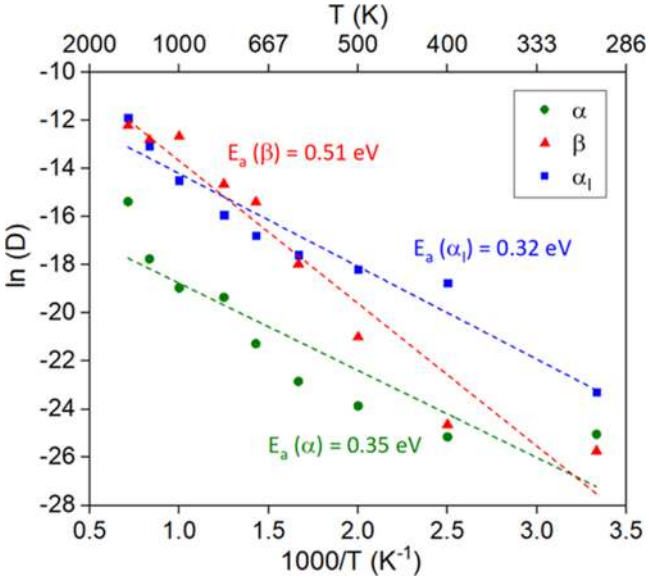

Figure 3. Arrhenius plot of Na-ion diffusion coefficients vs temperature for $NaVOPO_4$ polymorphs.

optimized structure to have vacancy concentrations of 0, 25, 50, 75, and 100%, and various vacancy configurations were considered. The voltage was then calculated using eq 1 with the lowest energy configuration. The computed voltages of the α-, β-, and α_I-$NaVOPO_4$ polymorphs are 3.3, 3.1, and 3.1 V (vs Na/Na^+), respectively. These are in good agreement with the experimental values of 3.6, 3.3−3.4, and 3.4 V (vs Na/Na^+), respectively.[14−16]

We have also investigated how doping on the vanadium site affects the cell voltage of the $NaVOPO_4$ polymorphs. The voltage trends of $NaV_{1-x}M_xOPO_4$ (M = Al^{3+}, Co^{2+}, Fe^{3+}, Mn^{4+}, Ni^{2+}, or Ti^{4+}) vs Na/Na^+ with *x* values of 0, 0.25, and 0.50 are depicted in Figure 5. These cations were chosen as they have been used as doping agents for different vanadium phosphate compounds, including $Li_3V_2(PO_4)_3$ and $Na_3V_2(PO_4)_3$.[56−64] The doped materials show higher capacity and capacity retention than the pristine compounds. Also, the addition of the cation dopants has been shown to enhance Li- and Na-ion diffusion, and have a structural stabilization effect.

Our computed cell voltage values of some of the doped structures are above the voltage stability window for organic

DOI: 10.1021/acs.jpcc.8b07797
J. Phys. Chem. C 2018, 122, 25829−25836

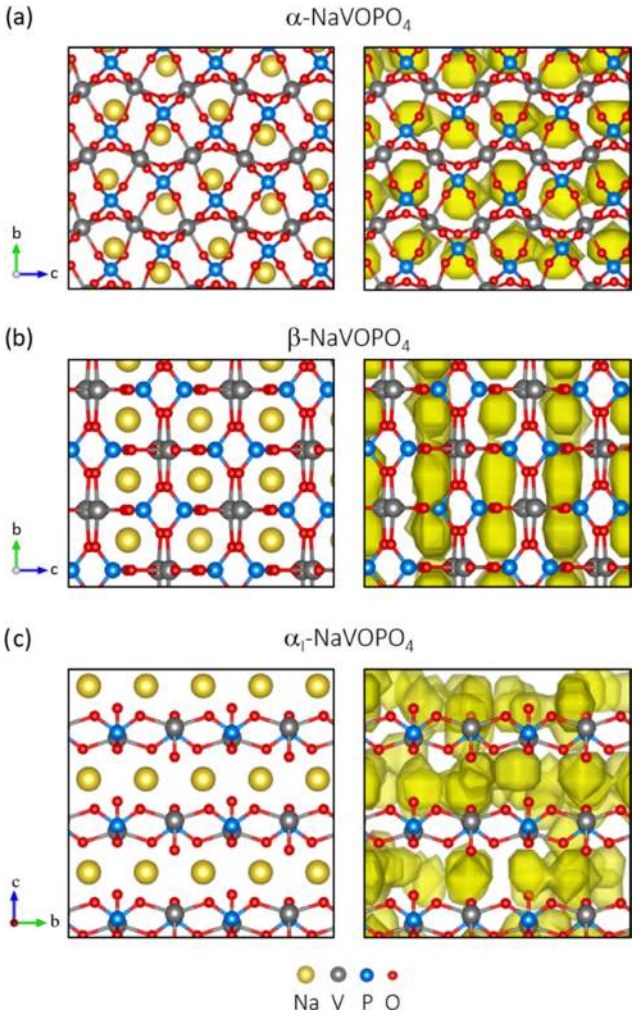

Figure 4. Na density plot from MD calculations at 700 K showing the initial structures (left) and Na diffusion pathways (right) of the (a) α-, (b) β-, and (c) α_I-$NaVOPO_4$ polymorph structures. Na-ion density is plotted in yellow.

Na-ion electrolytes (~3.5 V).[65] In the case of the α phase, the Co-, Mn-, and Ti-doped structures, when $x = 0.25$, are the only materials within this electrochemical window. When $x = 0.50$, all of the doped structures have cell voltage values above 3.5 V vs Na/Na^+. For the β phase, all of the doped structures ($x = 0.25$) are within the stability window, but only Mn- and Ti-doped structures ($x = 0.50$) have voltage values of ~3.5 V vs Na/Na^+. Finally, all of the doped α_I materials ($x = 0.25$ and 0.50) show computed voltages within the electrochemical stability window. We have also observed that in the doped systems, where the cation has a lower oxidation state than 4+, some of the vanadium centers are oxidized to V^{5+} to compensate for the charge. Overall, the Mn^{4+} and Ti^{4+} cations seem to be the more suitable dopants to increase the cell voltage of the $NaVOPO_4$ polymorphs within the optimal operating voltage window.

4. CONCLUSIONS

$NaVOPO_4$ vanadyl phosphates are among the most promising cathode materials for sodium-ion batteries because of their good electrochemical performance. We have studied the diffusion, electronic properties, and cation-doping behavior of the α-, β-, and α_I-$NaVOPO_4$ polymorphs. Our fundamental

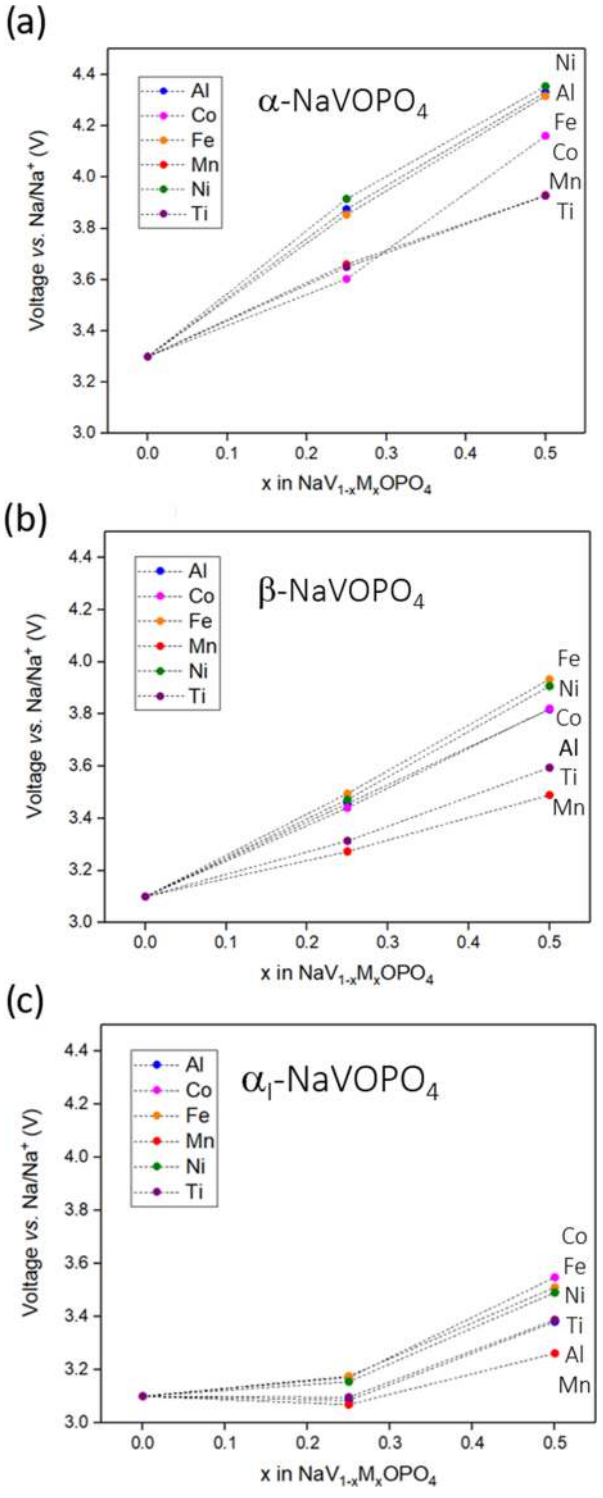

Figure 5. Trends in cell voltage (vs Na/Na^+) as a function of increasing dopant (M = Al^{3+}, Co^{2+}, Fe^{3+}, Mn^{4+}, Ni^{2+} or Ti^{4+}) concentration on the V site in the (a) α-, (b) β-, and (c) α_I-$NaVOPO_4$ polymorphs.

study shows good reproduction of the observed experimental structures. From large-scale MD calculations, we have derived low Na-ion activation energies of 0.3–0.5 eV, and diffusion coefficients (D_{Na}) at 300 K of 10^{-11}–10^{-12} cm^2 s^{-1} for the three $NaVOPO_4$ polymorphs. From analysis of the migration pathways, the α, β, and α_I phases show Na-ion diffusion along 2D, 1D, and 3D channels, respectively. Among the three

DOI: 10.1021/acs.jpcc.8b07797
J. Phys. Chem. C 2018, 122, 25829–25836

polymorphs, the α_I phase has the most favorable Na-ion conductivity, activation energy, and 3D pathways, making it a promising cathode material.

The computed cell voltages of 3.3, 3.1, and 3.1 V vs Na/Na^+ for the α-, β-, and α_I-$NaVOPO_4$ compounds, respectively, agree well with the reported electrochemical data. Cation doping (Al^{3+}, Co^{2+}, Fe^{3+}, Mn^{4+}, Ni^{2+}, and Ti^{4+}) at the vanadium site is predicted to increase the cell voltage. The Mn- and Ti-doped structures of the α and β phases show an increase in the cell voltage within the electrochemical stability window of current liquid electrolytes. In the case of the α_I phase, all of the doped structures show cell voltages within the electrochemical stability range. Overall, the fundamental insights presented in this study will aid the improvement of phosphate cathodes for sodium-ion batteries.

■ ASSOCIATED CONTENT

Supporting Information

The Supporting Information is available free of charge on the ACS Publications website at DOI: 10.1021/acs.jpcc.8b07797.

Density of states of β and α_I-(Na)$VOPO_4$ polymorphs, interatomic potential parameters table, computed and experimental bond lengths of the three polymorphs and polyhedral representation of the doped materials (PDF)

■ AUTHOR INFORMATION

Corresponding Authors

*E-mail: apariciosanchezp@cardiff.ac.uk (P.A.A.).
*E-mail: m.s.islam@bath.ac.uk (M.S.I.).
*E-mail: deleeuwn@cardiff.ac.uk (N.H.d.L.).

ORCID

Pablo A. Aparicio: 0000-0003-3719-7241
James A. Dawson: 0000-0002-3946-5337
M. Saiful Islam: 0000-0003-3882-0285
Nora H. de Leeuw: 0000-0002-8271-0545

Notes

The authors declare no competing financial interest.

■ ACKNOWLEDGMENTS

The authors acknowledge the Engineering and Physical Sciences Research Council (EPSRC) for financial support (Energy Materials Programme grant EP/K016288). We also acknowledge ARCHER HPC facilities and the Materials Chemistry Consortium (EPSRC grant EP/L000202). The authors acknowledge the use of HPC Wales for computing time. We would like to thank Dr Christopher Eames and Dr Piermanuele Canepa from the University of Bath and Prof Christian Masquelier from the University of Picardie for helpful discussions. All data created during this research are openly available from the Cardiff University's Research Portal at http://doi.org/10.17035/d.2018.0060727953.

■ REFERENCES

(1) Kundu, D.; Talaie, E.; Duffort, V.; Nazar, L. F. The Emerging Chemistry of Sodium Ion Batteries for Electrochemical Energy Storage. *Angew. Chem., Int. Ed.* **2015**, *54*, 3431−3448.

(2) Fang, C.; Huang, Y.; Zhang, W.; Han, J.; Deng, Z.; Cao, Y.; Yang, H. Routes to High Energy Cathodes of Sodium-Ion Batteries. *Adv. Energy Mater.* **2016**, *6*, No. 1501727.

(3) Kim, H.; Kim, H.; Ding, Z.; Lee, M. H.; Lim, K.; Yoon, G.; Kang, K. Recent Progress in Electrode Materials for Sodium-Ion Batteries. *Adv. Energy Mater.* **2016**, *6*, No. 1600943.

(4) Hwang, J.-Y.; Myung, S.-T.; Sun, Y.-K. Sodium-Ion Batteries: Present and Future. *Chem. Soc. Rev.* **2017**, *46*, 3529−3614.

(5) Ni, Q.; Bai, Y.; Wu, F.; Wu, C. Polyanion-Type Electrode Materials for Sodium-Ion Batteries. *Adv. Sci.* **2017**, *4*, No. 1600275.

(6) Yabuuchi, N.; Kubota, K.; Dahbi, M.; Komaba, S. Research Development on Sodium-Ion Batteries. *Chem. Rev.* **2014**, *114*, 11636−11682.

(7) Han, M. H.; Gonzalo, E.; Singh, G.; Rojo, T. A Comprehensive Review of Sodium Layered Oxides: Powerful Cathodes for Na-Ion Batteries. *Energy Environ. Sci.* **2015**, *8*, 81−102.

(8) Zhang, X.; Zhang, Z.; Yao, S.; Chen, A.; Zhao, X.; Zhou, Z. An Effective Method to Screen Sodium-Based Layered Materials for Sodium Ion Batteries. *npj Comput. Mater.* **2018**, *4*, No. 13.

(9) Li, F.; Zhou, Z. Micro/Nanostructured Materials for Sodium Ion Batteries and Capacitors. *Small* **2018**, *14*, No. 1702961.

(10) Lim, S. Y.; Kim, H.; Shakoor, R. A.; Jung, Y.; Choi, J. W. Electrochemical and Thermal Properties of NASICON Structured $Na_3V_2(PO_4)_3$ as a Sodium Rechargeable Battery Cathode: A Combined Experimental and Theoretical Study. *J. Electrochem. Soc.* **2012**, *159*, A1393−A1397.

(11) Shakoor, R. A.; Seo, D.-H.; Kim, H.; Park, Y.-U.; Kim, J.; Kim, S.-W.; Gwon, H.; Lee, S.; Kang, K. A Combined First Principles and Experimental Study on $Na_3V_2(PO_4)_2F_3$ for Rechargeable Na Batteries. *J. Mater. Chem.* **2012**, *22*, 20535−20541.

(12) Barker, J.; Saidi, M. Y.; Swoyer, J. L. A Sodium-Ion Cell Based on the Fluorophosphate Compound $NaVPO_4F$. *Electrochem. Solid-State Lett.* **2003**, *6*, A1−A4.

(13) Fang, Y.; Zhang, J.; Xiao, L.; Ai, X.; Cao, Y.; Yang, H. Phosphate Framework Electrode Materials for Sodium Ion Batteries. *Adv. Sci.* **2017**, *4*, No. 1600392.

(14) Song, J.; Xu, M.; Wang, L.; Goodenough, J. B. Exploration of $NaVOPO_4$ as a Cathode for a Na-Ion Battery. *Chem. Commun.* **2013**, *49*, 5280−5282.

(15) He, G.; Huq, A.; Kan, W. H.; Manthiram, A. β-$NaVOPO_4$ Obtained by a Low-Temperature Synthesis Process: A New 3.3 V Cathode for Sodium-Ion Batteries. *Chem. Mater.* **2016**, *28*, 1503−1512.

(16) He, G.; Kan, W. H.; Manthiram, A. A 3.4 V Layered $VOPO_4$ Cathode for Na-Ion Batteries. *Chem. Mater.* **2016**, *28*, 682−688.

(17) Li, H.; Peng, L.; Zhu, Y.; Chen, D.; Zhang, X.; Yu, G. An Advanced High-Energy Sodium-Ion Full Battery Based on Nanostructured $Na_2Ti_3O_7$/$VOPO_4$ Layered Materials. *Energy Environ. Sci.* **2016**, *9*, 3399−3405.

(18) Lin, Y.-C.; Hidalgo, M. F. V.; Chu, I.-H.; Chernova, N. A.; Whittingham, M. S.; Ong, S. P. Comparison of the Polymorphs of $VOPO_4$ as Multi-Electron Cathodes for Rechargeable Alkali-Ion Batteries. *J. Mater. Chem. A* **2017**, *5*, 17421−17431.

(19) Eames, C.; Clark, J. M.; Rousse, G.; Tarascon, J. M.; Islam, M. S. Lithium Migration Pathways and Van Der Waals Effects in the $LiFeSO_4OH$ Battery Material. *Chem. Mater.* **2014**, *26*, 3672−3678.

(20) Islam, M. S.; Fisher, C. A. J. Lithium and Sodium Battery Cathode Materials. Computational Insights into Voltage, Diffusion and Nanostructural Properties. *Chem. Soc. Rev.* **2014**, *43*, 185−204.

(21) Armstrong, A. R.; Lyness, C.; Panchmatia, P. M.; Islam, M. S.; Bruce, P. G. The Lithium Intercalation Process in the Low-Voltage Lithium Battery Anode $Li_{1+x}V_{1-x}O_2$. *Nat. Mater.* **2011**, *10*, 223−229.

(22) Yuan, Y.; Zhan, C.; He, K.; Chen, H.; Yao, W.; Sharifi-Asl, S.; Song, B.; Yang, Z.; Nie, A.; Luo, X.; et al. The Influence of Large Cations on the Electrochemical Properties of Tunnel-Structured Metal Oxides. *Nat. Commun.* **2016**, *7*, No. 13374.

(23) Clark, J. M.; Nishimura, S.; Yamada, A.; Islam, M. S. High-Voltage Pyrophosphate Cathode: Insights into Local Structure and Lithium-Diffusion Pathways. *Angew. Chem., Int. Ed.* **2012**, *51*, 13149−13153.

(24) Dawson, J. A.; Canepa, P.; Famprikis, T.; Masquelier, C.; Islam, M. S. Atomic-Scale Influence of Grain Boundaries on Li-Ion Conduction in Solid Electrolytes for All-Solid-State Batteries. *J. Am. Chem. Soc.* **2018**, *140*, 362−368.

DOI: 10.1021/acs.jpcc.8b07797
J. Phys. Chem. C 2018, 122, 25829−25836

(25) Dawson, J. A.; Attari, T. S.; Chen, H.; Emge, S. P.; Johnston, K. E.; Islam, M. S. Elucidating Lithium-Ion and Proton Dynamics in Anti-Perovskite Solid Electrolytes. *Energy Environ. Sci.* **2018**, *11*, 2993−3002.
(26) Kresse, G.; Hafner, J. Ab Initio Molecular Dynamics for Liquid Metals. *Phys. Rev. B* **1993**, *47*, 558−561.
(27) Kresse, G.; Hafner, J. Ab Initio Molecular-Dynamics Simulation of the Liquid-Metal-Amorphous-Semiconductor Transition in Germanium. *Phys. Rev. B* **1994**, *49*, 14251−14269.
(28) Kresse, G.; Furthmüller, J. Efficiency of Ab Initio Total Energy Calculations for Metals and Semiconductors Using a Plane-Wave Basis Set. *Comput. Mater. Sci.* **1996**, *6*, 15−50.
(29) Kresse, G.; Furthmüller, J. Efficient Iterative Schemes for Ab Initio Total-Energy Calculations Using a Plane-Wave Basis Set. *Phys. Rev. B* **1996**, *54*, 11169−11186.
(30) Blöchl, P. E. Projector Augmented-Wave Method. *Phys. Rev. B* **1994**, *50*, 17953−17979.
(31) Kresse, G.; Joubert, D. From Ultrasoft Pseudopotentials to the Projector Augmented-Wave Method. *Phys. Rev. B* **1999**, *59*, 1758−1775.
(32) Perdew, J. P.; Ruzsinszky, A.; Csonka, G. I.; Vydrov, O. A.; Scuseria, G. E.; Constantin, L. A.; Zhou, X.; Burke, K. Restoring the Density-Gradient Expansion for Exchange in Solids and Surfaces. *Phys. Rev. Lett.* **2008**, *100*, No. 136406.
(33) Tsirlin, A. A.; Nath, R.; Abakumov, A. M.; Furukawa, Y.; Johnston, D. C.; Hemmida, M.; Krug von Nidda, H.-A.; Loidl, A.; Geibel, C.; Rosner, H. Phase Separation and Frustrated Square Lattice Magnetism of $Na_{1.5}VOPO_4F_{0.5}$. *Phys. Rev. B* **2011**, *84*, No. 014429.
(34) Heath, J.; Chen, H.; Islam, M. S. $MgFeSiO_4$ as a Potential Cathode Material for Magnesium Batteries: Ion Diffusion Rates and Voltage Trends. *J. Mater. Chem. A* **2017**, *5*, 13161−13167.
(35) Grimme, S.; Antony, J.; Ehrlich, S.; Krieg, H. A Consistent and Accurate Ab Initio Parametrization of Density Functional Dispersion Correction (DFT-D) for the 94 Elements H-Pu. *J. Chem. Phys.* **2010**, *132*, No. 154104.
(36) Deng, Y.; Eames, C.; Nguyen, L. H. B.; Pecher, O.; Griffith, K. J.; Courty, M.; Fleutot, B.; Chotard, J.-N.; Grey, C. P.; Islam, M. S.; et al. Crystal Structures, Local Atomic Environments, and Ion Diffusion Mechanisms of Scandium-Substituted Sodium Superionic Conductor (NASICON) Solid Electrolytes. *Chem. Mater.* **2018**, *30*, 2618−2630.
(37) Deng, Y.; Eames, C.; Chotard, J.-N.; Lalère, F.; Seznec, V.; Emge, S.; Pecher, O.; Grey, C. P.; Masquelier, C.; Islam, M. S. Structural and Mechanistic Insights into Fast Lithium-Ion Conduction in Li_4SiO_4−Li_3PO_4 Solid Electrolytes. *J. Am. Chem. Soc.* **2015**, *137*, 9136−9145.
(38) Fisher, C. A. J.; Kuganathan, N.; Islam, M. S. Defect Chemistry and Lithium-Ion Migration in Polymorphs of the Cathode Material Li_2MnSiO_4. *J. Mater. Chem. A* **2013**, *1*, 4207−4214.
(39) Plimpton, S. Fast Parallel Algorithms for Short-Range Molecular Dynamics. *J. Comput. Phys.* **1995**, *117*, 1−19.
(40) Lii, K. H.; Li, C. H.; Chen, T. M.; Wang, S. L. Synthesis and Structural Characterization of Sodium Vanadyl(IV) Orthophosphate $NaVOPO_4$. *Z. Kristallogr. - Cryst. Mater.* **1991**, *197*, 67−73.
(41) O'Connor, C. J.; Soghomonian, V.; Haushalter, R. C.; Wang, Z.; Zubieta, J. One-Dimensional Antiferromagnetic Behavior in $AVOPO_4$ (A = NH_4, Na) Prepared from Hydrothermal Conditions. *J. Appl. Phys.* **1994**, *75*, 5859−5861.
(42) Amorós, P.; Marcos, M. D.; Roca, M.; Alamo, J.; Beltrán-Porter, A.; Beltrán-Porter, D. Crystal Structure of a New Polytype in the V−P−O System: Is ω-$VOPO_4$ a Dynamically Stabilised Metastable Network? *J. Phys. Chem. Solids* **2001**, *62*, 1393−1399.
(43) Girgsdies, F.; Schneider, M.; Brückner, A.; Ressler, T.; Schlögl, R. The Crystal Structure of δ-$VOPO_4$ and Its Relationship to ω-$VOPO_4$. *Solid State Sci.* **2009**, *11*, 1258−1264.
(44) Bordes, E. Crystallochemistry of V-P-O Phases and Application to Catalysis. *Catal. Today* **1987**, *1*, 499−526.
(45) Girgsdies, F.; Dong, W.-S.; Bartley, J. K.; Hutchings, G. J.; Schlögl, R.; Ressler, T. The Crystal Structure of ε-$VOPO_4$. *Solid State Sci.* **2006**, *8*, 807−812.
(46) Dupré, N.; Wallez, G.; Gaubicher, J.; Quarton, M. Phase Transition Induced by Lithium Insertion in α_I- and α_{II}-$VOPO_4$. *J. Solid State Chem.* **2004**, *177*, 2896−2902.
(47) Dupré, N.; Gaubicher, J.; Le Mercier, T.; Wallez, G.; Angenault, J.; Quarton, M. Positive Electrode Materials for Lithium Batteries Based on $VOPO_4$. *Solid State Ionics* **2001**, *140*, 209−221.
(48) Lim, S. C.; Vaughey, J. T.; Harrison, W. T. A.; Dussack, L. L.; Jacobson, A. J.; Johnson, J. W. Redox Transformations of Simple Vanadium Phosphates: The Synthesis of ε-$VOPO_4$. *Solid State Ionics* **1996**, *84*, 219−226.
(49) Sun, W.; Du, J. Structural Stability, Electronic and Thermodynamic Properties of $VOPO_4$ Polymorphs from DFT+U Calculations. *Comput. Mater. Sci.* **2017**, *126*, 326−335.
(50) Mueller, T.; Hautier, G.; Jain, A.; Ceder, G. Evaluation of Tavorite-Structured Cathode Materials for Lithium-Ion Batteries Using High-Throughput Computing. *Chem. Mater.* **2011**, *23*, 3854−3862.
(51) Matts, I. L.; Dacek, S.; Pietrzak, T. K.; Malik, R.; Ceder, G. Explaining Performance-Limiting Mechanisms in Fluorophosphate Na-Ion Battery Cathodes through Inactive Transition-Metal Mixing and First-Principles Mobility Calculations. *Chem. Mater.* **2015**, *27*, 6008−6015.
(52) Shibata, T.; Kobayashi, W.; Moritomo, Y. Sodium Ion Diffusion in Layered Na_xCoO_2. *Appl. Phys. Express* **2013**, *6*, No. 097101.
(53) Shibata, T.; Kobayashi, W.; Moritomo, Y. Sodium Ion Diffusion in Layered Na_xMnO_2 ($0.49 \leq x \leq 0.75$): Comparison with Na_xCoO_2. *Appl. Phys. Express* **2014**, *7*, No. 067101.
(54) Treacher, J. C.; Wood, S. M.; Islam, M. S.; Kendrick, E. Na_2CoSiO_4 as a Cathode Material for Sodium-Ion Batteries: Structure, Electrochemistry and Diffusion Pathways. *Phys. Chem. Chem. Phys.* **2016**, *18*, 32744−32752.
(55) Geifman, I. N.; Nagorniy, P. G.; Rotenfeld, M. V. EPR of V^{4+} in Lithium (Sodium) and Titanium Oxyphosphate and Superionic Conductivity of These Single Crystals. *Ferroelectrics* **1997**, *192*, 87−91.
(56) Ren, M.; Zhou, Z.; Li, Y.; Gao, X. P.; Yan, J. Preparation and Electrochemical Studies of Fe-Doped $Li_3V_2(PO_4)_3$ Cathode Materials for Lithium-Ion Batteries. *J. Power Sources* **2006**, *162*, 1357−1362.
(57) Kuang, Q.; Zhao, Y.; An, X.; Liu, J.; Dong, Y.; Chen, L. Synthesis and Electrochemical Properties of Co-Doped $Li_3V_2(PO_4)_3$ Cathode Materials for Lithium-Ion Batteries. *Electrochim. Acta* **2010**, *55*, 1575−1581.
(58) Deng, C.; Zhang, S.; Yang, S. Y.; Gao, Y.; Wu, B.; Ma, L.; Fu, B. L.; Wu, Q.; Liu, F. L. Effects of Ti and Mg Codoping on the Electrochemical Performance of $Li_3V_2(PO_4)_3$ Cathode Material for Lithium-Ion Batteries. *J. Phys. Chem. C* **2011**, *115*, 15048−15056.
(59) Zhang, Y.; Huo, Q.; Lv, Y.; Wang, L.; Zhang, A.; Song, Y.; Li, G.; Gao, H.; Xia, T.; Dong, H. Effects of Nickel-Doped Lithium Vanadium Phosphate on the Performance of Lithium-Ion Batteries. *J. Alloys Compd.* **2012**, *542*, 187−191.
(60) Zhang, L.-L.; Liang, G.; Peng, G.; Huang, Y.-H.; Wang, L.; Qie, L.; Croft, M. C.; Ignatov, A.; Goodenough, J. B. Insight into Fe Incorporation in $Li_3V_2(PO_4)_3$/C Cathode Material. *J. Electrochem. Soc.* **2012**, *159*, A1573−A1578.
(61) Tao, D.; Wang, S.; Liu, Y.; Dai, Y.; Yu, J.; Lei, X. Lithium Vanadium Phosphate as Cathode Material for Lithium Ion Batteries. *Ionics* **2015**, *21*, 1201−1239.
(62) Lai, C.; Chen, Z.; Zhou, H.; Lu, Y.; Li, H. Mn-Doped $Li_3V_2(PO_4)_3$ Nanocrystal with Enhanced Electrochemical Properties Based on Aerosol Synthesis Method. *J. Mater. Sci.* **2015**, *50*, 3075−3082.
(63) Sun, H.-B.; Zhang, L.-L.; Yang, X.-L.; Liang, G.; Li, Z. Investigation of Co-Incorporated Pristine and Fe-Doped $Li_3V_2(PO_4)_3$ Cathode Materials for Lithium-Ion Batteries. *Dalton Trans.* **2016**, *45*, 15317−15325.

DOI: 10.1021/acs.jpcc.8b07797
J. Phys. Chem. C 2018, 122, 25829−25836

(64) Zhang, B.; Chen, H.; Tong, H.; Wang, X.; Zheng, J.; Yu, W.; Zhang, J.; Li, J.; Zhang, W. Synthesis and Electrochemical Performance of Ni Doped $Na_3V_2(PO_4)_3$/C Cathode Materials for Sodium-Ion Batteries. *J. Alloys Compd.* **2017**, *728*, 976−983.
(65) Ponrouch, A.; Dedryvere, R.; Monti, D.; Demet, A. E.; Ateba Mba, J. M.; Croguennec, L.; Masquelier, C.; Johansson, P.; Palacin, M. R. Towards High Energy Density Sodium Ion Batteries through Electrolyte Optimization. *Energy Environ. Sci.* **2013**, *6*, 2361−2369.

DOI: 10.1021/acs.jpcc.8b07797
J. Phys. Chem. C 2018, 122, 25829−25836